Environmental Earth Sciences (2019) 78:608
https://doi.org/10.1007/s12665-019-8622-4

ORIGINAL ARTICLE

Groundwater systems in bare and covered karst aquifers: evidence from tracer tests, hydrochemistry, and groundwater ages

Guanghui Jiang[1] · **Fang Guo**[1] · **Changyuan Tang**[2]

Received: 5 September 2018 / Accepted: 27 September 2019 / Published online: 11 October 2019

Abstract

The east Guilin region contains a karst dominated hydrological system along the Lijiang River. The two main topographic characteristics of the basin are peak cluster depression and peak forest. Despite the fact that these areas represent adjacent units, they have different groundwater movement patterns. This study describes the groundwater and solute movement in the different hydrogeological sub-regions via several techniques. Our results indicated that the topographic boundary between the peak cluster depression and the peak forest is clear. However, a transition zone exists between these topographic zones, and it can be determined in terms of groundwater movement. We employed several methods that are widely considered to be effective. Tracer tests were conducted in the transition zone, hydrochemistry techniques were used in the peak forest, and groundwater age dating based on CFCs was employed throughout the study area. The main conduits could be found in the transition zone, but the groundwater flow was much slower in the transition zone than in the mountain peak cluster area. Minor conduits also accounted for a high proportion of the total flow in the transition zone. The solute migration within the plain, which was determined by analyzing the nitrates, was controlled by mixing and distance effects. The maximum nitrate concentration was limited at the local scale. The nitrate concentration gradient at the regional scale was not related to the groundwater movement, indicating that the groundwater recharged in a dispersed manner and discharged at discrete locations along the river. The age dating revealed that the groundwater was older in the plain than in the bare mountain zone. This was due to the strong mixing of young and old water, which was the result of the characteristics of the karst media in the aquifer. Our investigation of the groundwater system in a bare/covered karst aquifer provides data for decision-making in effective groundwater management.

Keywords Fengcong and Fenglin · Groundwater system · Groundwater age · Pollutant transport · Guilin

Introduction

Karst covers approximately one-third of the Chinese territory. The southern China karst region extends over half a million km^2, mainly in Yunnan, Guizhou, and Guangxi provinces. Peak cluster (Fengcong) depressions and peak forest (Fenglin) plains are two typical types of karst landforms in southern China (Zhu 1982). These types correspond to bare and covered karst aquifers (karst covered by loose sediments), respectively (Yuan et al. 1991). In peak cluster depression areas, the rock surface of the bare karst develops karrens and sinkholes. These features enhance the concentrated recharge. The karst conduit network collects the runoff, and then, intense discharge occurs via springs. In contrast, karst aquifers in peak forests receive decentralized recharge through fractures, resulting in dispersed discharge. In comparison to bare karst aquifers, covered karst aquifers in southern China usually lack subterranean rivers. In covered karts areas, surface karst formations, such as sinkholes and karst windows, are absent. In addition, the relatively thick soil covering makes it difficult to determine the runoff processes (Guo et al. 2002, 2013). The clarification of the flow processes in covered karst areas is a difficult topic

✉ Fang Guo
gfkarst@126.com

Guanghui Jiang
bmnxz@126.com

Changyuan Tang
tangchy3@mail.sysu.edu.cn

[1] Key Laboratory of Karst Dynamics, MNR/GZAR, Institute of Karst Geology, CAGS, Guilin 541004, China

[2] Chiba University, Matsudo 271-8510, Japan

in hydrogeology research. Since the terrain is normally flat in covered karst areas and the land resources are abundant, peak forest plains are usually distributed in areas with large human populations. In peak forest plains, karst groundwater is abundant. However, the groundwater exploitation intensity is quite large. Because there is a significant level of human activity in these areas, the risk of groundwater pollution is high. Sustainable utilization of groundwater resources and the protection of water resources both require an understanding of the groundwater distribution and the characteristics of the flow path.

Concerns regarding groundwater movement in karst areas have been raised throughout the world (Goldscheider and Drew 2007). Karst aquifers are highly heterogeneous complex systems. This complexity is due to the high spatial variability of their three types of porosity: rock matrix porosity, fracture porosity, and conduit porosity (Ford and Williams 2007). These aquifers typically exhibit dual groundwater flow regimes, i.e., fast (conduit dominated) flow and slow (diffuse) flow. Groundwater collects in and flows through conduits and fractures (Kaufmann and Braun 2000). Karst topography is well developed in most areas of southern China. At present, 3066 subterranean rivers have been discovered and cataloged. The underground system is the main pattern of the groundwater movement. These groundwater systems usually have clear discharge outlets, and many only have a single outlet. Therefore, the internal features and the runoff process can be investigated using tracer tests, hydrographs, and chemograph analysis (Jiang et al. 2015a, b). Although conduit flow and fracture flow coexist in covered karst aquifers, backbone conduits and concentrated discharge outlets are absent. Therefore, it is difficult to determine the flow pathway at the catchment scale. Under these circumstances, multiple techniques are required to determine and verify the flow paths.

Hydrochemistry, isotope tracers, dye tracer tests, and groundwater dating are effective techniques for studying groundwater flow and solute and pollutant transport in aquifers (Geyer et al. 2013). Hydrochemical data can be used to directly determine the water quality, and the monitoring equipment is fairly easy to install. However, it cannot determine groundwater flow and associated contaminant migration within the aquifer. Tracer tests have obtained good results in conduit dominated water systems in bare mountain areas, but this technique faces unsolved problems in other karst water systems. For instance, dye tracer tests in water systems with no obvious main conduit, but a good porosity and homogeneous water distribution, produce unsatisfactory results. Despite the rapid groundwater flow potential of karst aquifers, contaminants can reside in an aquifer for a long time prior to being transported. This potential for a lag effect represents one limitation of using tracer testing to determine how pollutants are transported. Groundwater ages, which can be used as an indicator of residence time, can provide the actual time required for recharge water introduced into the system to reach the saturated aquifer (Zoellmann et al. 2001). The groundwater residence time can be determined using environmental tracers, including ^{14}C, CFCs (chlorofluorocarbons), SF_6 (sulfur hexafluoride), ^{3}H–^{3}He, and ^{85}kr, which are all common tracers used in groundwater dating (Plummer et al. 2001). The presence of ^{14}C is used to detect old water, while CFCs and SF_6 are used to assess younger waters (up to 60 years old). Based on the SF_6 contents, the age of the groundwater in the karst depressions was estimated to be 10 years, while the age of water from the outlet of spring S31 at the Yaji karst experiment site was estimated to be 8 years (Li et al. 2007). Groundwater ages estimated from CFCs are useful for locating karst conduits (Long and Putnam 2006); however, groundwater dating using these tracer gases is seldom reported for karst groundwater systems in southern China where karst is highly developed. A combined of multi-techniques with new method might help to develop a conceptual model or understand karst structure in this typical covered karst aquifer.

The purpose of this study is to describe the groundwater flow process in two neighboring, but distinct, geomorphic karst water systems using multiple techniques. Specifically, we discuss how to choose appropriate research techniques and methods, including dye tracer tests, hydrochemistry, and groundwater ages, based on the hydrogeologic conditions of the sub-regions. Dye tracer tests are used to investigate the main conduit flow and to calculate the groundwater's flow velocity. Based on a nitrate case study, the evolution of solute and its relationship to the groundwater flow in the plain is discussed. CFCs are used as an indicator of groundwater age in an attempt to estimate the residence time of groundwater in the aquifer. Groundwater velocity, solute migration within the groundwater, and the groundwater's age are used to obtain a better understanding of the groundwater runoff patterns in the fragile karst aquifer. This knowledge will aid pollution treatment and effective water management of the aquifer.

Study area

The east Guilin region is located in the east of the Lijiang River, which is one of the most famous karst landscapes in the world. The east Guilin region is an integrated hydrogeological unit with an area of 136 km^2 (Fig. 1). Groundwater from the karst aquifer of east Guilin supplies much of the domestic and industrial water consumption in this region via private extraction. This region is located in the suburban region outside of the Guilin city. Various polluting activities occur in this area, including excrement from pigs and other animals. Livestock are poorly managed and roam freely

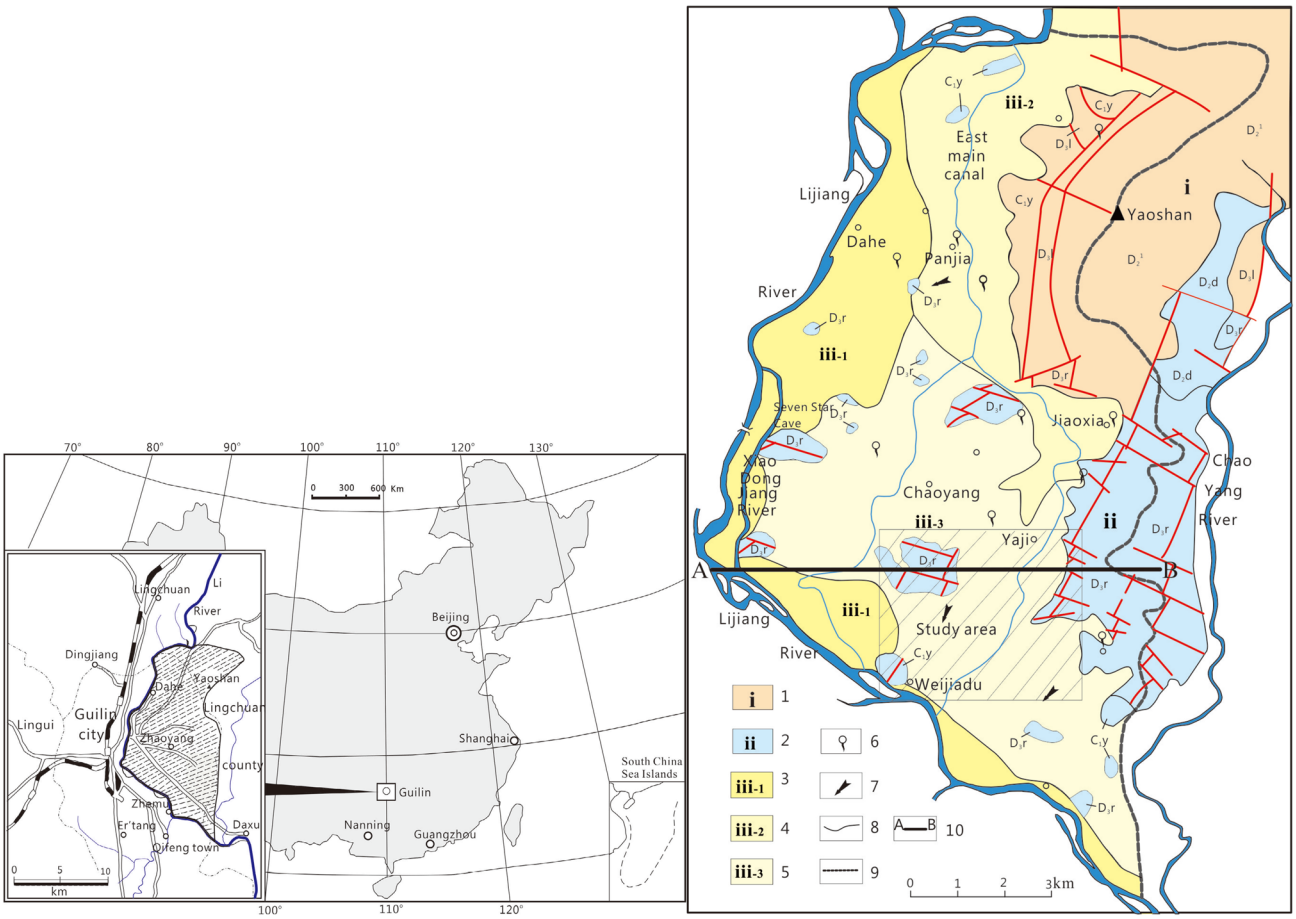

Fig. 1 Location and simple regional hydrogeologic map of the east Guilin region. (1) Yaoshan clastic rock area, pore water in the clastic rocks and impure carbonate; (2) peak cluster area, bare karst water; (3) peak forest area, pore water in the upper alluvium layer, karst water in the lower layer; (4) peak forest area, pore water in the upper diluvium layer, karst water in the lower layer; (5) peak forest area, red clay gravel layer in the upper layer, karst water in the lower layer; (6) karst spring; (7) groundwater flow direction; (8) the boundary of the karst hydrogeological zone; (9) the boundary of the groundwater watershed; (10) hydrogeological profile (see Fig. 2)

throughout this rural area. The agricultural activity mainly entails farming vegetables, rice, and other dry crops. The industry is primarily composed of small individual plants, such as factories that produce rubber products, bricks, and tiles. The scale of the industrial land use has gradually increased in recent years, resulting in the decline and disappearance of natural forests. The groundwater pollution in this area leads to decreased groundwater quality, affects the usefulness of the water supply, and influences the water quality of the Lijiang River.

The east Guilin region has a typical subtropical monsoon climate with hot, wet summers and mild, dry winters. The mean annual precipitation is 1949 mm, and the mean average evaporation is 1697 mm according to data from National Meteorological Information Center of China. The average annual air temperature is 18.9 °C with a maximum mean value of 23 °C in August and a minimum mean value of 15.6 °C in January.

The topography of the east Guilin region is characterized by high elevations in the east and low elevations in the west. Yaoshan Mountain, which is the highest mountain in the area, is located in the northeastern part of the study area. It has an elevation of 990 m and is composed of sandstone bedrock. The Lijiang River is the base level for both surface water and groundwater in this area. Two tributaries of the Lijiang River, the Xiao Dong Jiang River and the Chao Yang River, are located in this region. The eastern main canal of a reservoir in the north flows through the entire region from north to south. Along this flow path, water infiltrates to recharge to the aquifer. Thick, pure carbonate rock is well developed in the region, including the upper Devonian Rongxian (D_3r) and Guilin formations (D_3g) and the middle Devonian Donggangling (D_2d) Formation.

According to the topographic and hydrogeological conditions, the hydrogeologic features in the east Guilin region can be divided into three categories (Fig. 1). Sub-region (1)

includes the Yaoshan clastic rocks and accounts for 14% of the total area. Groundwater collects in the near-surface structural fractures and in the weathering fissure zones. Sub-region (2) includes the peak clusters and accounts for 10% of the total area. The bedrock is mainly composed of carbonate rock. The soil cover is very thin and most of the bedrock is bare. The karst features are well developed with a high density of caves and depressions, which serve as recharge points for precipitation and play a key role in the groundwater cycle. The bottom of the peak cluster depression is approximately 150 m a.s.l. Sub-region (3) includes the peak forest and accounts for 76% of the total area. This sub-region is mostly covered by Quaternary deposits, except for a small proportion of bare karst. In addition to the Lijiang River, there is pore water in the upper layer and karst water in the lower layer. In other regions, the karst water is covered by clay. Detailed groundwater-level monitoring was conducted across the basin in the late 1980 s, and since then, the ongoing investigation of the aquifer has revealed that the groundwater flow is generally from northeast to southwest, i.e., towards the Lijiang River (Fig. 2).

A 60 km^2 area in sub-regions ii and iii was selected as the study area (Fig. 3). Even though the study area is only part of the hydrogeologic unit, it is a large enough part to allow us to gain an understanding of the hydrogeologic characteristics and the related behavior of contaminates in the aquifer. The study area (referred to hereafter as the east Guilin region) is characterized by gray–brown and abilene sandy clay with pH values ranging from 4.5 to 6.5. The covering soil is usually thin, i.e., a mean thickness of less than 1 m, in the bare mountain area. In the plains, the covering layer can be relatively thick, ranging from 1–28 m. Caves can be found in almost every peak. Fissures, karst conduits, and caves are the main storage and flow paths for the groundwater. The karst water is primarily recharged by rainfall. The water level does not vary significantly with changes in the base level of the river or the topography. In the plains, shallow groundwater is usually found at depths of 2–5 m. Karst groundwater movement mainly occurs in the horizontal direction over 10 km; therefore, the rate of groundwater circulation is usually slow. Due to the shallow water levels and the existence of foot caves (horizontal caves that develop along the groundwater table) at the foot of the isolated peaks in the peak forest (Fig. 4), wastewater from human activities can easily flow into the karst aquifer.

There are some natural outcrops of karst groundwater in this aquifer, including springs, foot caves, blue holes, and solution caves. In addition, groundwater has been exposed by artificial drilling, including wells and boreholes. The wells and boreholes are mostly located in the villages and suburbs. Most of the wells have been abandoned due to groundwater pollution or the provision of tap water.

The study area includes two types of karst landform, with different hydrogeologic conditions. From the view of hydrogeology, the study area can be divided into bare mountain zone (I), transition zone (II), and plain zone (III) (Fig. 3).

Methods

Previous studies have showed dye tracer tests can be used to clearly trace the path of the underground streams in this area (Jiang et al. 2016). However, hydrochemistry methods are not applicable due to the high heterogeneity of the karst

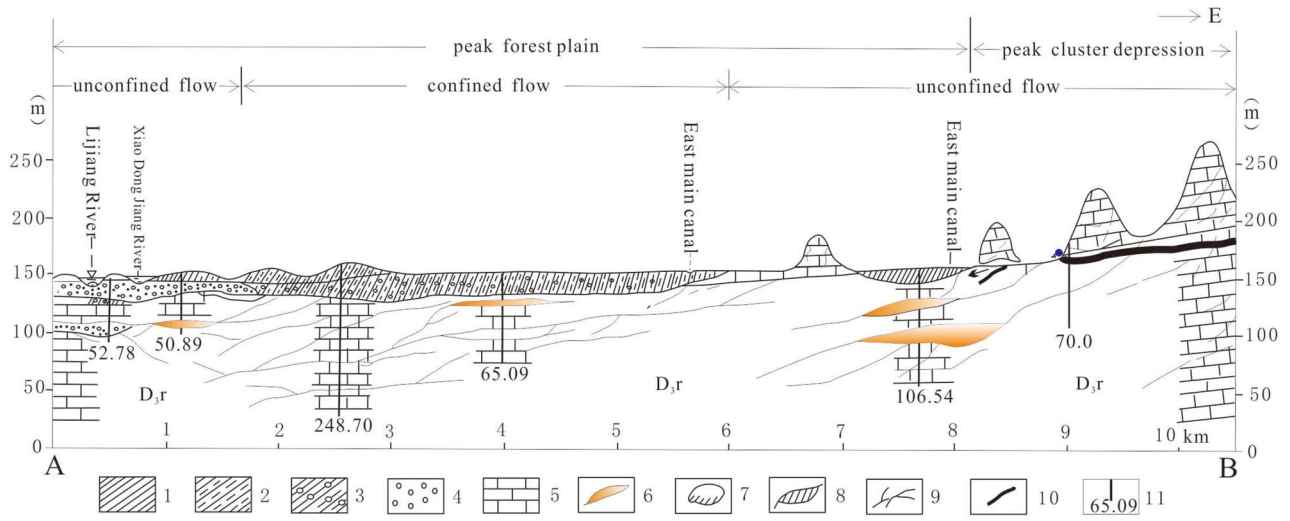

Fig. 2 Hydrogeological profile of the study area. (1) clay; (2) mild clay; (3) gravel layer; (4) sand and gravel layer; (5) Devonian D_3r Formation; (6) cave; (7) half-filled cave; (8) filled cave; (9) solution fissure; (10) karst conduit; (11) borehole (up: number; down: depth in meters)

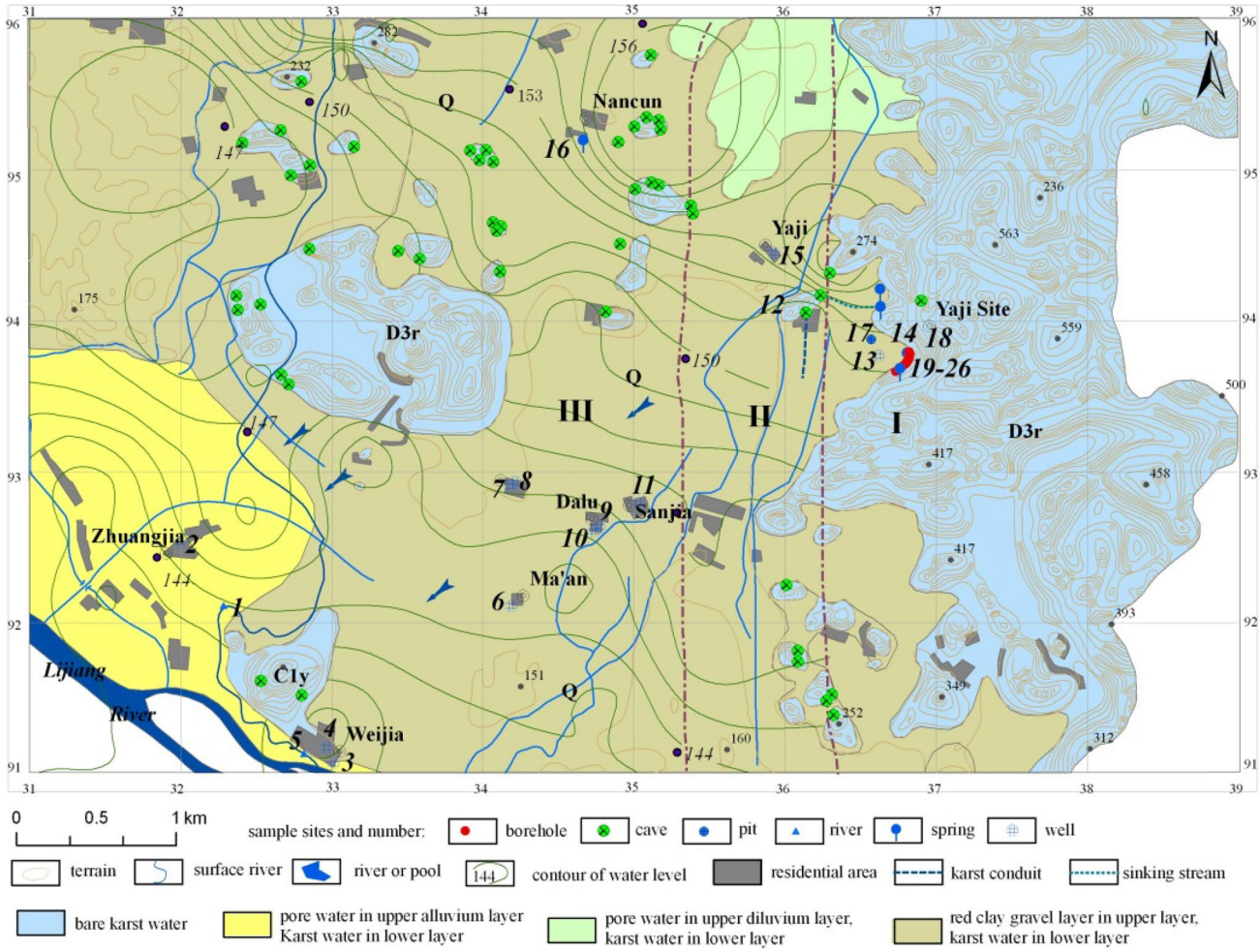

Fig. 3 General groundwater flow direction in the study area and sample sites. Sample site numbers: (1) ZJR; (2) ZJT; (3) WJT; (4) WJY; (5) WJR; (6) MAW; (7) JBY; (8) JBT; (9) DLG; (10) DLR; (11) SJS; (12) MAF; (13) YJD; (14) S31; (15) YJY; (16) NCS; (17) GSW; (18) CF1; (19) KF1; (20) KF2; (21) KF3; (22) KF4; (23) KF5; (24) KF6; (25) KF7; (26) KF8; (27) KF9. I: bare mountain zone; II: transition zone; III: plain zone

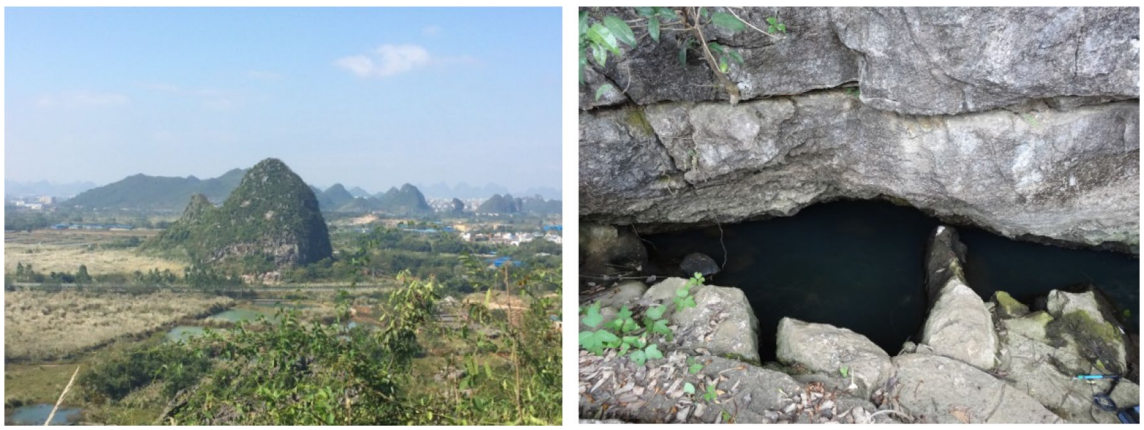

Fig. 4 Karst features in the study area (left: peak forest plain; right: foot cave in an isolated peak)

media. Dye tracer tests are the most effective method in the transition zone, even though the results may not be satisfactory. This is because the groundwater collects in both conduits and fractures. Dye tracer tests are completely inapplicable in the plain zone, but hydrochemistry techniques might produce good results in this zone. As a new technique in karst hydrology, groundwater dating was used throughout the study area. The Yaji karst hydrogeology experiment site (Yaji site) is located in the bare mountain zone. The continuous monitoring and research conducted at the Yaji site since 1986 has provided a sufficient understanding of the hydrogeologic background and groundwater movements of the area (Yuan et al. 1990). Therefore, this area is not the focus of this study.

Sample collection and analysis

Hydrochemistry data from 2009 to 2013 were available for the east Guilin region. Groundwater samples were collected from springs, caves, foot caves, blue holes, and wells. Some of the water collection points were repeatedly sampled during this 5 year period. Before the water was collected, the pH, water temperature, dissolved oxygen (DO), oxidation–reduction potential (ORP), and electrical conductivity were measured on site using a WTW Cond 3420. The water samples were taken to the laboratory for major anion and cation analyses. Hydrochemistry plays an important role in groundwater movement determination due to the distribution and transport of contaminants. Nitrate (NO_3^-) was selected as the contaminant indicator. Nitrate was chosen, because it is a common contaminant in groundwater. In addition, it is introduced into the aquifer by human activities, allowing it to serve as an artificial tracer.

Each sampling site was located using GPS, and was recorded along with number, date, well depth, the main land use, and any other pertinent site data. The samples for major cation and anion analysis were filtered through a 0.45 μm membrane and collected in plastic bottles. The samples were transported to the laboratory and stored at 4 °C in a refrigerator. The cations were analyzed using an ICP-OES (Perkin-Elme Company). The anions were analyzed using Ion Chromatography (Dionex ICS3000). All of the ion analyses were performed at the Analytical Center of the Institute of Karst Geology in Guilin, China.

Groundwater dye tracer tests

Tracer tests were carried out twice, in November 2009 and in November 2011. Both of the tracer tests were conducted during the dry season. The first tracer test was conducted over a short distance within 446 m and within a small area (1.5 km^2), while the second tracer test was conducted over a large distance of 10 km and within a large area (extending to the Lijiang River).

Spring S31 (No. 14 in Fig. 2), which is a perennial spring with an average flow rate of 4 L/s, is a groundwater discharge outlet in the bare mountain zone. Before the tests were conducted, the injection and collection points were sampled to obtain background values.

In the first test, 400 g of uranine were injected into a swallow hole 50 m from spring S31. Eight collection points (labeled A–H) were established at wells and pools that were distributed approximately 500 m downstream from the injection point. The water was sampled every other day for a total of 2 months.

In the second test, 2 kg of uranine were injected at a depth of 10 m in cave S31. Thirty-three collection points were set in canals, pools, caves, and wells at nearby groundwater points between the injection points to the area near the Lijiang River. The points spanned a total distance of approximately 10 km. The water was sampled every day in the beginning of the first month. Then, the sampling was changed to a several day interval. The sampling took place over a 4 month period. The uranine concentration was determined in the laboratory using a fluorescence flowmeter with a precision of 0.02×10^{-6} ppm.

The collection points of the two tests were established at wells, pools, caves, and other groundwater exposed points. Measurement for the groundwater velocity was inaccessible. Therefore, the recovery rate of tracer could not be calculated. The aims of dye tracer tests in this paper were limited to discuss the possibility of groundwater flow from the bare karst aquifer to the plain.

Groundwater age dating

As was mentioned in the introduction, there are several short-term residence indicators. Each indicator has advantages and disadvantages (Hinsby et al. 2001). CFCs are the only indicator used in this study, because SF_6 could not be used, since limestone releases it into the groundwater, resulting in younger ages. Furthermore, the use of CFCs was sufficient to meet our objectives, and thus, even though $^3He/^2He$ would also be suitable, it was not used.

26 karst water points including 1 cave, 2 springs, 14 wells, and 9 boreholes in the Yaji site were sampled for CFC dating in December 2012.

Brown glass bottles (100 ml) were pre-cleaned by heating them at 450 °C for 2 h to prevent contamination. Then, these bottles were used for the CFC sampling. A submersible stainless-steel bottle was used to hold the 100 ml bottles. After the bottles were submerged in the flowing water, the valve was closed to avoid air contamination. The CFC concentrations were determined using gas chromatography (GC-ECD, Electron Capture Detector; GC-14B, SHIMADZU),

in the Laboratory of the Graduate School of Horticulture, Chiba University, Japan. The limit of detection was 0.01 pmol/kg and the measured precision was 1%. The CFC concentrations were obtained via chromatographic analysis and were reported in pmol/kg. These values were converted to atmospheric mixing ratios (pptv) according to the estimated recharge temperature and altitude. Then, the recharge year and apparent ages were evaluated using an Excel program developed by the USGS (http://water.usgs.gov/lab/).

The apparent age of the sampled water was determined by comparing the partial pressures of the CFC compounds. The partial pressures were calculated from the measured concentrations using the solubility data for each compound in conjunction with the record of CFCs in North America at different times. Several basic conditions were assumed in these calculations. The potential for biological, geochemical, and hydrologic processes to alter the CFC concentrations of the aquifer is the most important assumption. The DO and ORP were used to determine the potential geochemical alteration of the CFCs. DO controls the solubility of many naturally occurring elements, including trace elements in groundwater (Rose and Long 1988a, b). The DO of the samples ranged from 1.5 to 8.0 mg/L, indicating an oxygen-rich environment. The ORP is another important parameters used to characterize oxygen-rich environments in groundwater systems. It controls the speciation of many molecules as well as geochemically and microbially mediated transformations within the system (Thayalakumaran et al. 2008). The samples for the ORP analysis were collected in the east Guilin region in December 2012 concurrently with the CFC samples.

Results

Dye tracer tests to identify groundwater flow

Eight sampling sites labeled A–H were set for the first tracer test. The connections of these groundwater sites from different sampling locations with the spring were expected to judge. And if they were connected, comparison of results could help to distinguish the primary and secondary flow pathways. A and B are surface pools; C, D, E (YJD, No. 13 in Fig. 2), F, and G are shallow groundwater wells; and H is a karst window. Uranine was detected at sites A, B, C, D, E, F, and G. Sites E and G had the highest concentrations and the longest duration time. Sites E and G are considered to represent the main flow path. Uranine was not detected at site H. Although uranine was detected at sites C, D, and F, these sites had very low concentrations and short time durations. Therefore, they are considered to represent the minor flow paths (Fig. 5). According to the variation in the concentration of the uranine at sites E and G, the average velocity of the groundwater is 21 m/day.

The second tracer test was carried out over a much larger area and a longer distance, i.e., from the foot of the peak cluster to the Lijiang River. Thirty-three collection points were set. The collection points included springs, wells, foot caves, channels, pools, and surface rivers, covering almost all of the outcropping water in this zone. 22 days after injection, the tracer was detected and gradually increased at site YJD (Fig. 6). The uranine concentration continued to increase for almost 3 months, confirming that this is one of the main channels of the groundwater flow path from the bare mountain zone to the transition zone. The average flow velocity was 85 m/day based on the uranine variation at site YJD.

Site GSW is a blue hole located 50 m from site YJD. At the beginning of the 106 day experimental period, no tracer was detected at site GSW. On day 107, the concentration of uranine increased to 1.26 ppb. 10 days later, it dropped to 0.11 ppb. According to the meteorological data for this area, there were a total of 51.3 mm of rainfall during the tracer test. Before this, six rainfall events occurred, which each exceeded 10 mm.

Except for sites YJD and GSW, none of the collection points experienced distinct changes in their uranine concentrations. In other words, no clear results were obtained for these collection points.

Hydrochemistry in the peak forest plain

Fourteen water samples, including samples from springs, wells, and surface water, are plotted in Fig. 7. These water samples were collected in June 2012. The nitrate concentrations range from 7.16 to 206.82 mg/L. The 25% quantile threshold is 15.64 mg/L, the median is 39.38 mg/L, and the 75% quantile threshold is 120.02 mg/L. The nitrate content can be divided into four categories based on statistics. The first category includes the values between the minimum value and the 25% quantile cutoff. The second, third, and fourth categories include the values from the 25% quantile to the median, the median to the 75% quantile threshold, and the 75% quantile cutoff to the maximum value, respectively (Fig. 7). Four samples fall into the first category, three samples fall into the second category, three samples fall into the third category, and four samples fall into the fourth category.

All of the water samples in the plain zone, including samples from the 1980 s, 2009, 2012, 2013, 2014, and 2015, were incorporated into a box-plot (Fig. 8). We found that the average concentration of NO_3^- in the 1980 s was only 11.08 mg/L, while the average values of nitrate in 2009, 2012, 2013, 2014, and 2015 were 20.78, 52.33, 80.44, 24.06, and 24.40 mg/L, respectively. In general, the average nitrate content in the present stage is two-to-eight times higher than

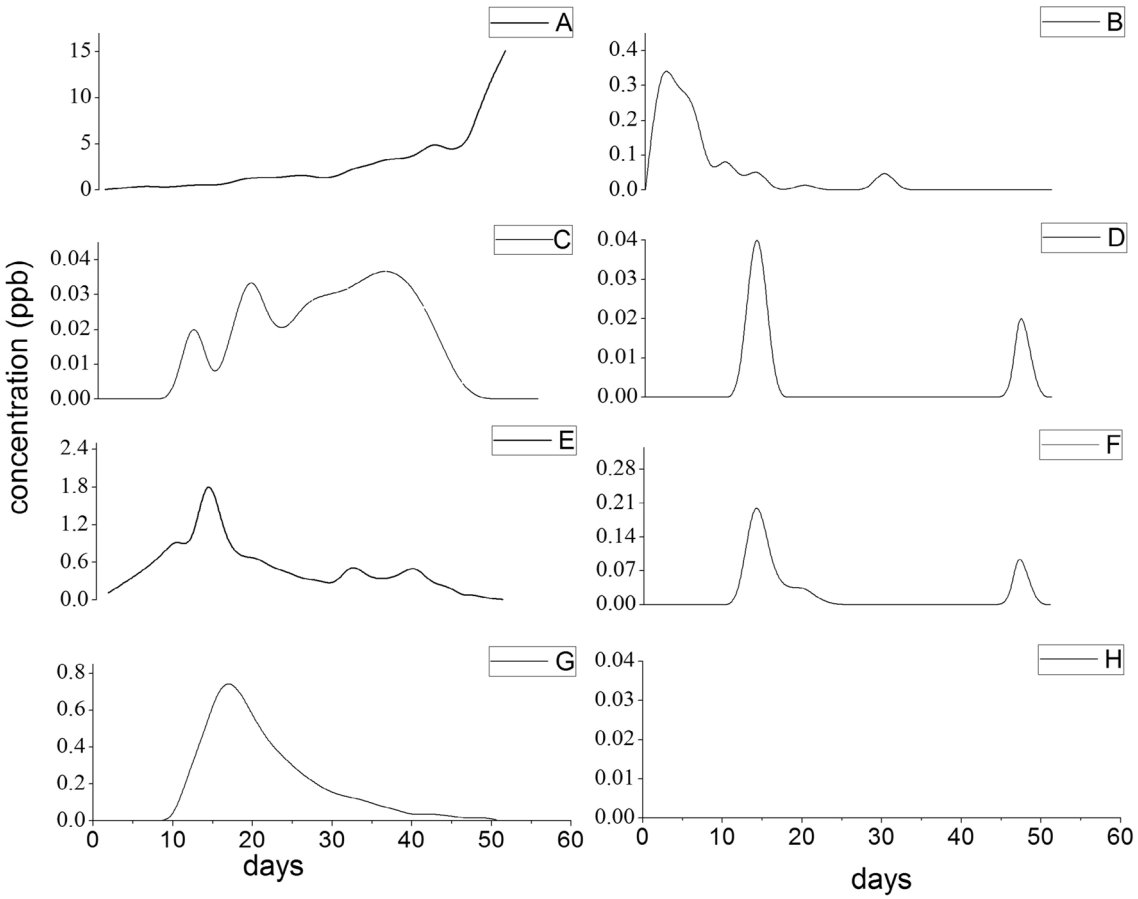

Fig. 5 Results of the first tracer test (not in the same scale; plots order alphabetically)

the values in the 1980 s. The nitrate content from 2012 to 2013 is the highest in this time series. After 2014, the nitrate content decreased.

Several factors can affect nitrate content in the aquifer in different years. The intensity of human activities, the amount of domestic sewage input, and the precipitation are in the lists. Besides, the temporal variability of nitrate should be considered (Huebsch et al. 2014). Some of the water samples in Fig. 8 were sampled monthly during 2014 and 2015. For example, the standard deviation of nitrate contents in site GSW and site NCS were 3.75 and 3.23, indicating that the annual variances were small.

Apparent groundwater ages

These DO values of these samples ranged from 2 to 7.6 mg/L, and the ORP levels ranged from 129 to 235 mV. DO levels above 1 mg/L and ORP values of 150–500 mV suggest an anoxic environment (Millero 1986); therefore, our results indicate that the groundwater system in the east Guilin region has an aerobic environment. Hence, reduction would not occur in this groundwater environment, indicating water was under aerobic condition and CFCs should not be affected by microbial degradation (Hinsby et al. 2007). Therefore, it is reasonable to use CFCs as a groundwater age indicator in this aquifer.

The CFC concentrations of the groundwater varied from 0.13 to 147.92 pmol/kg for CFC-12, from 1.05 to 1040.02 pmol/kg for CFC-11, and from 0.06 to 0.33 pmol/kg for CFC-113. Table 1 shows the apparent ages from the binary mixing model (BMM). It was assumed that each spring is a simple mixture of recently recharged water from a shallow flow system with older water from a deeper flow system (Happell et al. 2006). Using these assumptions, the fraction of post 1993 water can be calculated from each CFC concentration as has been done by Katz et al. (2001). Several studies have reported the CFC sequence of degradation to be CFC11 → CFC113 → CFC12 (Höhener et al. 2003). Therefore, CFC-12 is considered to be the most stable and the most resistant to degradation. Based on the hydrogeological background of the area and the validation of the CFC concentrations, we concluded that the BMM provides the best results for this indicator. The apparent ages of the CFC-12 concentrations calculated using BMM varied from

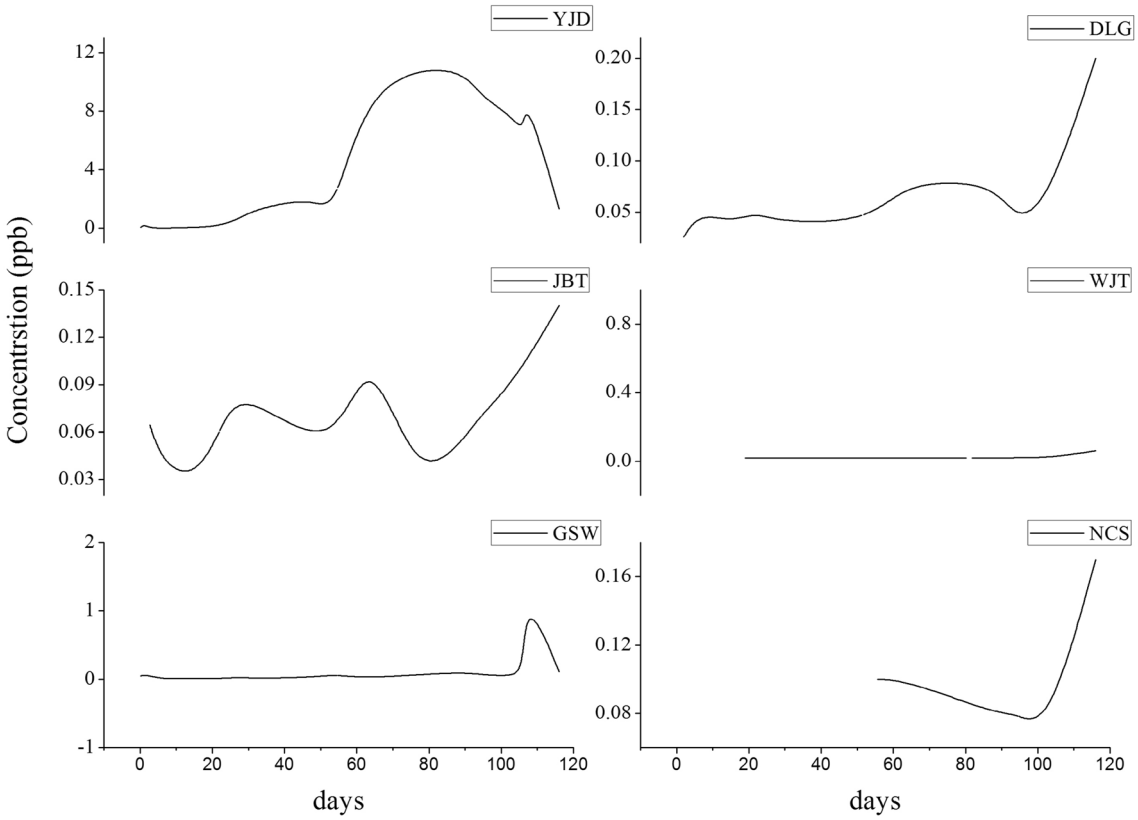

Fig. 6 Results of the second tracer test (not in the same scale)

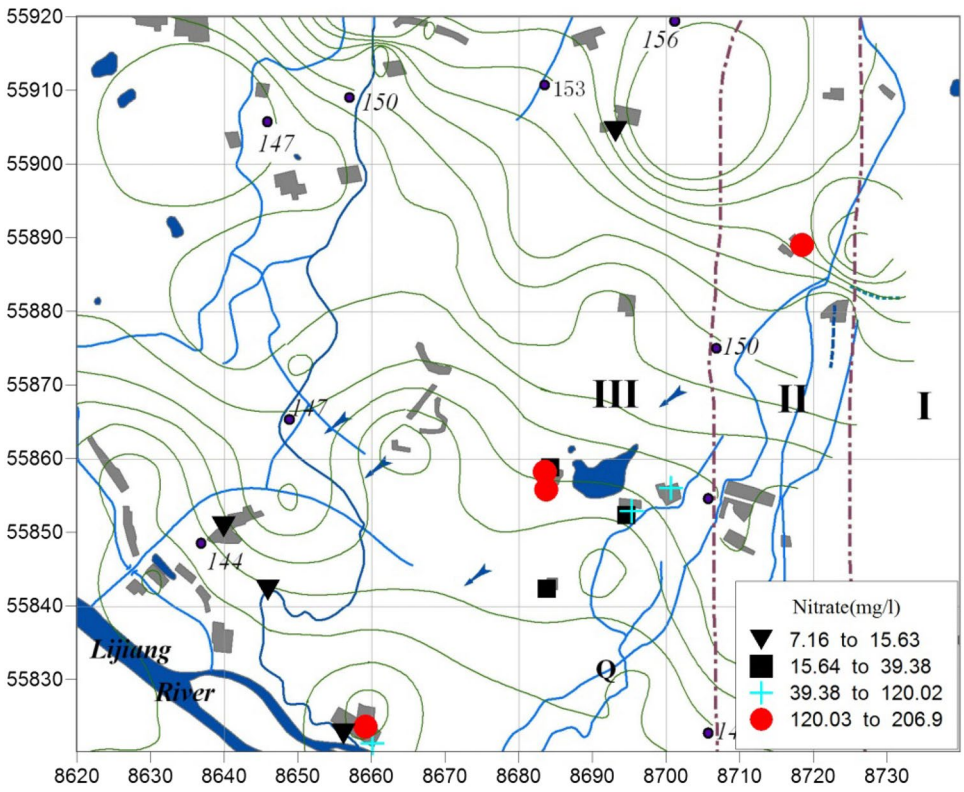

Fig. 7 Spatial distribution of nitrate concentrations in the plain

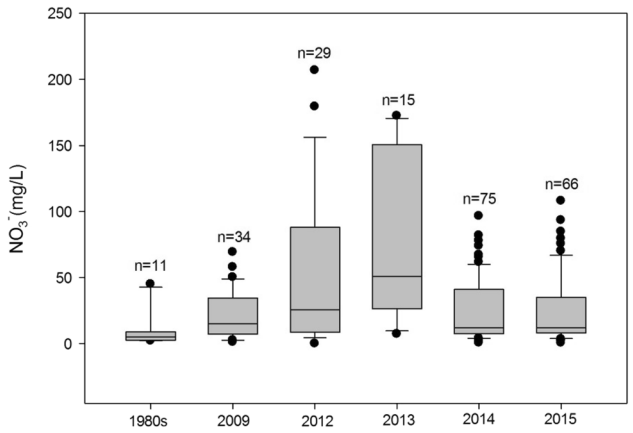

Fig. 8 Box-plot of the nitrate concentrations from the 1980 s to 2015

33 to 52 years (Table 1) with an average age of 39.5 years. The average age of the groundwater is 38 years in the transition zone and 44 years in the plain. Not all of the CFC apparent ages were concordant. There were discrepancies of 3–10 years between the CFC12 and CFC113 ages. This is similar to the results of a recent study of an aquifer system in the Sacramento Mountains, USA (Land and Timmons 2016).

Discussion

Groundwater flow in the bare mountain zone

The Yaji karst experiment site is located in the bare mountain zone in the western part of the study area. The total area of the site is only 2 km^2; however, it has a complete water system, which includes four main sub-systems. Spring system S31 is the largest of the four subsystems. Continuous research in this area since 1986 has determined the characteristics of the groundwater flow and movement. Depression No. 1 is the only recharge area in spring system S31. The karst media in spring system S31 are dominated by conduit flow, with less dominant diffuse flow occurring in fractures

Table 1 CFCs' concentrations and calculated ages by BMM

Name	CFC-12 (pmol/kg)	CFC-11 (pmol/kg)	CFC-113 (pmol/kg)	Apparent age (years)			Ratio age (yrs)	Hydrogeological sub-region
				CFC-11	CFC-12	CFC-113	F113/F12	
CF1	0.76	142.15	0.10	M	38	31	26	Bare mountain zone
KF1	0.77	667.72	0.10	M	38	32	27	
KF2	0.52	71.23	0.07	C	42	34	26	
KF3	0.82	1040.02	0.09	M	37	33	29	
KF4	0.62	200.21	0.09	M	40	33	25	
KF5	0.64	78.42	0.08	C	40	33	26	
KF6	0.66	72.83	0.10	C	40	32	24	
KF7	0.65	88.31	0.07	C	40	35	29	
KF8	0.73	640.77	0.10	M	39	32	26	
KF9	0.70	170.59	0.07	M	39	34	29	
S31	0.49	168.49	0.10	M	42	31	NP	
MAF	0.58	52.70	0.09	C	41	32	23	Transition zone
GSW	1.07	934.23	0.12	M	33	30	28	
YJD	0.59	88.62	0.07	C	41	34	27	
YJY	147.92	164.39	0.27	M	M	23	NP	Plain zone
NCS	0.76	23.77	0.29	C	38	22	NP	
DLG	0.38	3.47	0.09	19	44	32	NP	
DLR	0.37	4.53	0.09	C	45	33	NP	
SJS	0.14	684.70	0.33	M	52	17	NP	
JBT	0.63	13.21	0.07	C	40	35	29	
JBY	0.13	36.16	0.06	C	52	36	NP	
MAW	0.52	46.97	0.09	C	42	33	21	
ZJT	0.39	1.05	0.07	41	44	35	21	
WJT	0.47	44.43	0.09	C	43	33	21	
WJY	0.50	7.13	0.10	C	42	32	21	

The CFC concentrations of the water samples are higher than the values in equilibrium with the 2013 atmospheric concentrations

C contaminated, *NP* age calculation not possible due to likely contamination, *yrs* years before sample dating, *M* modern, age is close to zero

and dissolution fissures (Yuan et al. 1996). From depression No. 1 to the outlet of spring system S31, the minimum groundwater flow velocity is 100 m/day during the dry season and the maximum flow velocity is 6000 m/day during the rainy season.

Determination of groundwater flow in the covered karst plain zone

Dye tracer tests have produced good results in bare mountain zones. However, this method may have some disadvantages in the transition zone and in the plain area. The soil covering in the transition zone is thin, and the karst surface formation is still developing. In the transition zone, groundwater from the bare mountain zone is transported into the plain zone. Based on two dye tracer tests, we determined the groundwater flow pathway. The main groundwater flow channel was identified as the collection point that contained high levels of the tracer over a long period of time. Collection points E and G fit this criterion. The collection points that did not receive the tracer have no connection or a poor connection. For example, collection point H in the first tracer test and point WJT in the second tracer test fit this description. Collection points that receive the tracer but exhibit low concentrations over a short period of time are considered to be minor channels. For instance, collection points C, D, and F in the first tracer test are minor channels. Collection points A and B may have received the tracer. However, they were sampled from surface water pools and the algae and organic matter may have affected the uranine measurements. The dye tracer tests show that the groundwater flows through the high permeability zone in the karst aquifer. Therefore, the tracer tests identify the groundwater movement direction and the high permeability of the runoff zone. The groundwater flow velocity is quite slow in the plain zone. The groundwater flow is restricted by the hydraulic slope. Therefore, the diffusion of the tracers is limited under these conditions. In contrast, the tracers become concentrated in the high permeability zone.

The results of the dye tracer tests in the transition zone indicate a close relationship with rainfall. More specifically, the results of the tracer tests are related to the groundwater level. Both tracer tests were conducted during the dry season. However, the total rainfall was small during the experimental period in 2009. The total rainfall during the 51-day experimental period was only 72.4 mm. In contrast, a total of 313.7 mm of rainfall occurred during the second tracer test. During the late stage of the second experiment, the groundwater level rose noticeably. This was reflected by the groundwater flow velocity. From site S31 to site YJD, the average flow velocity in the main runoff zone was 21 m/day in 2009, while it was 85 m/day in 2012. Five rainfall events occurred during the first 100 days of the second tracer test, but none of the rainfall events exceeded 10 mm. During this period, the tracer was not detected at site GSW. After 140.8 mm of rainfall, a tracer concentration of 1.26 ppb was detected. Despite the fact that site YJD is much closer to site GSW, the groundwater from site YJD does not flow to site GSW when the groundwater level is low. However, they are connected when the groundwater level is high.

In addition, most of the collection points in the plain zone did not receive the tracer in the second test. This does not mean that they are not connected. The artificial tracer test may have a certain range of application. Jiang et al. (2016) reported that the distance between the injection and collection points should not exceed 1 km to ensure good test results. For a distance of greater than 1 km, the tracer could be degraded due to the high porosity of the carbonate rocks and the slow groundwater flow velocity in the aquifer.

The hydrochemistry analysis, using nitrate as an indicator, showed that the contaminant did not have an effect on the accumulation or distinct diffusion direction along the groundwater flow paths. Therefore, hydrochemistry alone cannot be used to form a complete understanding of the karst media in the plain zone. Spatially, the nitrate concentration is mainly related to the pollution sources. The pollution is not serious, and the karst aquifer has a certain purification ability (Guo et al. 2014). The interaction between the surface water and the groundwater in the plain zone increases the transfer of nitrate. High nitrate contents are usually located near villages due to domestic sewage sources.

The nitrate concentration time series clearly shows the impact of human activities. Since 1950, industry has developed rapidly in Guilin. Guilin became a tourist city in the early 1980s. At that time, almost all of the factories were shut down and waste water treatment plants were built. The nitrate concentrations were lowest in the 1980s and the highest in 2012 and 2013. This indicates that the accumulation and degeneration of pollutants in the aquifer has a delayed effect. Groundwater runoff patterns determine the movement and diffusion of pollution in karst aquifers.

Some literatures have been discussed the importance of conduit–matrix interaction on solute transport (e.g. Faulkner et al. 2009). This study area has been divided into three parts according to the hydrogeology features. Karst conduit has been verified in the sub-region I, while there is no conduit in the sub-region III. Groundwater flows from the sub-region I to the sub-region III. Different from the laboratory analog, the interaction of conduit and matrix could not find in this scale. The evolution of the hydrochemistry in this covered karst aquifer is the result of two effects. The interaction between groundwater and surface water produces a mixing effect. Since the movement of groundwater is slow in the plain zone, the accumulation and release of pollutants is also a gradual process. Soil covering, good porosity of carbonate rocks, and the presence of foot caves in the karst plain

enhance the mixing effect. Distance effects are present in the relationship between the contaminant concentrations and the pollution sources. Shorter distances are related to higher pollution concentrations, indicating regional groundwater diffusion and transportation effects.

Tracer tests and the groundwater residence time in the aquifer

The results from CFC-11, CFC-12, and CFC-113 were not consistent with each other for any of the samples. This lack of concordance was most likely the result of the mixing of groundwater in the aquifer. Based on this hypothesis, binary mixing models were applied to calculate the degree to which young water was mixing into the aquifer due to a recent recharge event. The contribution of the younger water ranged from 22 to 80% for the 18 samples (Fig. 9). Site GSW is a blue hole located in the peak forest zone, 500 m from the piedmont of the peak cluster. This blue hole and the surrounding area usually flood in the rainy season. Therefore, site GSW had the highest percentage of young water among the samples. The other water samples from the plain contain 22% to 50% young water. Karst conduits can provide short-circuit pathways within an aquifer, which can result in groundwater mixtures of significantly different mean ages (Jurgens et al. 2012).

A direct correlation ($R^2 = 0.992$) was found between the apparent age of the water samples and the fraction of young water, with the oldest samples having the smallest percentage of young water (Fig. 10). This correlation suggested that the binary mixing model is valid. It also showed that

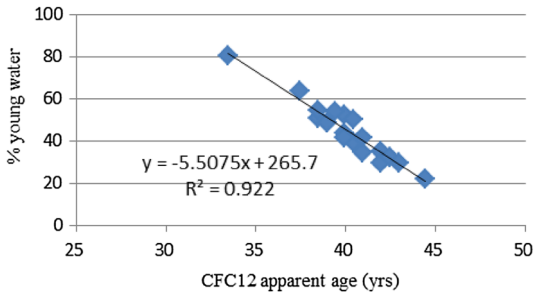

Fig. 10 CFC12 apparent age of the groundwater compared with the percent of young water in the samples

the percentage of young water is the main factor affecting the groundwater ages (Land and Timmons 2016). The age of a sample may be influenced by water mixing due to conduit/fracture/matrix interactions. The age can also be influenced by the mixing of groundwater from multiple sources (Land and Huff 2010). This phenomenon has been observed in other studies of dual porosity systems (e.g., Long et al. 2008). The sources of the mixing endmembers are recent recharge originating from precipitation and from older groundwater stored within the matrix.

The tracer tests indicate that the groundwater flow velocity is rapid in the bare mountain zone. In the karst plain zone, the flow velocity is 21 m/day for low groundwater levels and 85 m/day for high groundwater levels. In contrast to the dye tracer tests, which give high groundwater flow velocities in some parts of the water system, the apparent ages of the groundwater in the covered karst aquifer range from 33 to 52 years. The contradiction between the two techniques

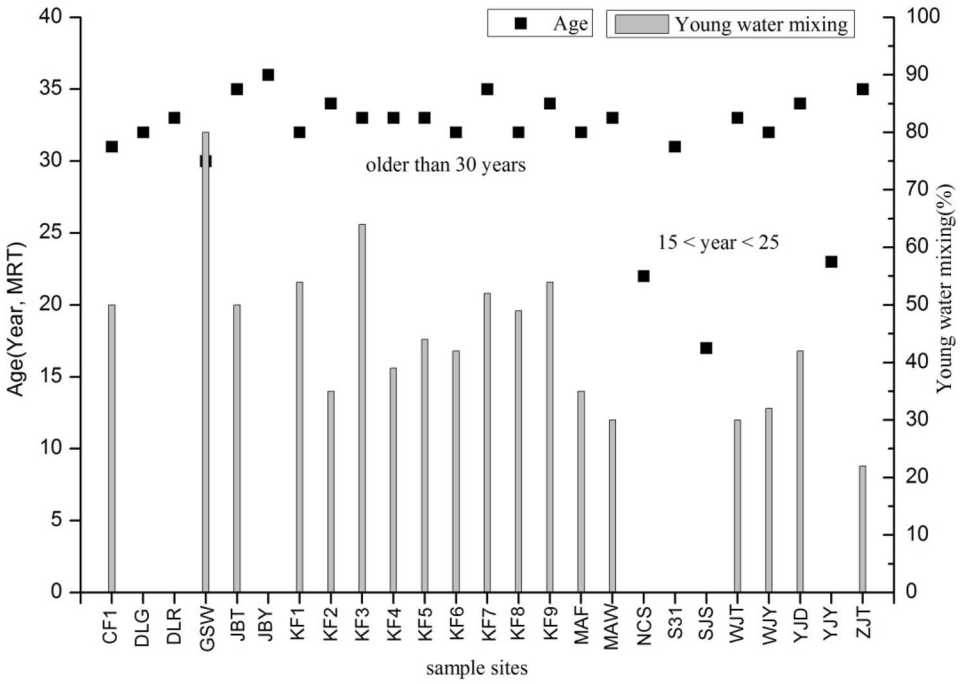

Fig. 9 Groundwater apparent ages and young water mixing (%)

was likely due to the nature of karst aquifers. Except for S31, NCS, and SJS, the other water samples for CFCs analysis were collected from karst fracture water. Fracture water was strongly mixing by the interaction of conduit and matrix. The tracer test can only measure the most rapidly moving water in the aquifer. However, the groundwater in the aquifer is recharged by mixing processes. In addition to fast flow in sinkholes and karst conduits, slow flow through soil seepage or fractures also occurs. In addition, groundwater resources are highly abundant in the peak forest-plain zone, which has a small hydrologic slope and a slow flow velocity. Therefore, the groundwater is old. Even though the bare karst mountain zone is dominated by conduits, fracture flow still plays an important role. This results in older groundwater ages in this area, as well.

In addition, the apparent age (or the transit time) of the water may not necessarily represent the age of the contamination. This is also caused by the mixing process occurring among the karst conduits, fractures, and matrix. Given that the groundwater transit times are on the order of decades and are related to the prolonged input of pollutants from multiple sources, pollutants could remain in a groundwater aquifer for several days, weeks, or decades (Katz et al. 2001). In contrast to the solute pattern, the contaminant levels are affected by the pollution input patterns and the mixing processes in the aquifer (Morales et al. 2017). The pattern of pollution is determined by the inputs and the groundwater ages, while the mixing processes induce the dilution or transfer of the pollution in the aquifer. Thus, high pollution contents may be the result of strong pollution inputs or the result of slow groundwater exchange and update. Low contaminant contents can be the result of weak pollution inputs or strong mixing processes in the aquifer (i.e., younger groundwater ages). Therefore, studies that attempt to understand the behavior of contaminates or to predict the pollution trends in karst aquifers should not overlook the groundwater flow structure.

Conclusions

In the bare-covered karst area, the groundwater flow system is difficult to determine. Techniques including tracer tests, hydrochemistry, and age dating were applied based on the specific hydrogeological conditions. Combined with the flow regime obtained from the groundwater level, a greater understanding of the karst groundwater flow pathways was generated.

In the bare mountain zone, the karst media are dominated by the conduit network. Sinkholes are common in the depression area. Groundwater discharge occurs through concentrated spring outlets. Age dating based on CFCs indicates that the groundwater is old, ranging from 37 to 40 years. The part of the groundwater that moves quickly can be measured using the tracer test. Fracture flow is quite slow in the bare karst mountain, which resulted in a higher total age.

The dye tracer tests indicate that the groundwater movement slows in the transition zone. The lower boundary of the breakthrough curve of the tracer ends at 2 months. Although the concentrated flow still represents a high percentage of the total flow in the zone, the discharge is not concentrated.

In the peak forest-plain zone, the groundwater is mainly recharged by diffuse flow. The overburden thickness is large, the hydraulic slope is small, and the water yield is good. Aquifers with larger capacities take longer to renew. Overall, within the water system, the groundwater is the oldest.

This attempt of multiple techniques application helps to understand the groundwater flow process in two neighboring but distinct geomorphic karst water systems. However, there are still some questions need to be concerned in the future research. In where complex hydrology combined by conduit flow and fracture flow exists, the real meaning of CFCS apparent ages of groundwater is still vague. The contradiction between CFCs and dye tracer test needs to be verified, and the impact of hydrogeology condition on CFCs is needed to be addressed by more tests.

Acknowledgements This study was funded by the National Natural Science Foundation of China (41772269) and the Key Research and Development Program of Guangxi (AB18221093). The authors would like to thank Dr. Han Zhiwei for his help with the laboratory analyses. We would like to thank the reviewers who read the first draft of this paper for their constructive comments. We would also like to thank LetPub (www.letpub.com) for providing linguistic assistance during the preparation of this manuscript.

References

Faulkner J, Hu BX, Kish S, Hua F (2009) Laboratory analog and numerical study of groundwater flow and solute transport in a karst aquifer with conduit and matrix domains. J Contam Hydrol 110(1–2):34–44

Ford DC, Williams P (2007) Karst hydrogeology and geomorphology. Wiley, New York

Geyer T, Birk S, Reimann T, Dörfliger N, Sauter M (2013) Differentiated characterization of karst aquifers: some contributions. Carbonates Evaporites 28(1–2):41–46

Goldscheider N, Drew D (2007) Methods in karst hydrogeology. Taylor & Francis, London

Guo F, Jiang GH, Pei JG, Zhang C (2002) Assessment on the water qualities of major subterranean rivers in Guangxi and their changing trend. Carsologica Sin 21(3):195–201

Guo F, Jiang GH, Yuan DX, Polk J (2013) Evolution of major environmental geological problems in karst areas of Southwestern China. Environ Earth Sci 69:2427–2435

Guo F, Wang WK, Jiang GH, Ma ZJ (2014) Contaminant transport behavior in a karst subterranean river and its capacity of self-purification: a case study of Lihu, Guangxi. Adv Water Sci 25(3):414–419

Happell JD, Opsahl S, Top Z, Chanton JP (2006) Apparent CFC and 3H/3He age differences in water from Floridan Aquifer springs. J Hydrol 319:410–426

Hinsby K, Edmunds WM, Loosli HH, Manzano M, Melo M, Barbecot F (2001) The modern water interface: recognition, protection and development-advance of modern waters in European aquifer systems. In: Edmunds WM, Milne CJ (eds) Palaeowaters in coastal Europe: evolution of groundwater since the Late Pleistocene, vol 189. Geological Society, London, pp 271–288

Hinsby K, Højberg AL, Engesgaard P, Jensen KH, Larsen F, Plummer L, Busenberg E (2007) Transport and degradation of chlorofluorocarbons (CFCs) in the pyritic Rabis Creek aquifer, Denmark. Water Resour Res 43(10):W10423

Höhener P, Duwig C, Pasteris G, Kaufmann K, Dakhel N, Harms H (2003) Biodegradation of petroleum hydrocarbon vapors: laboratory studies on rates and kinetics in unsaturated alluvial sand. J Contam Hydrol 66(1–2):93–115

Huebsch M, Fenton O, Horan B, Hennessy D, Richards KG, Jordan P, Goldscheider N, Butscher C, Blum P (2014) Mobilisation or dilution? Nitrate response of karst springs to high rainfall events. Hydrol Earth Syst Sci 11(4):216–226

Jiang GH, Guo F, Polk SJ, Kang ZQ, Wu JC (2015a) Delineating vulnerability of karst aquifers using hydrochemical tracers in Southwestern China. Environ Earth Sci 74:1015–1027

Jiang GH, Guo F, Yu S (2015b) Chemographs of karst water system and its new application in hydrogeological survey. J Jilin Univ Earth Sci Ed 45(3):899–907

Jiang GH, Guo F, Tang QJ, Li X, Zeng XR (2016) Application of tracer test techniques in hydrogeological survey in karst area. J Nanjing Univ (Nat Sci) 52(3):503–511

Jurgens BC, Böhlke JK, Eberts SM (2012) TracerLPM (version 1): An excel workbook for interpreting groundwater age distributions from environmental tracer data. US Geol Surv techniques methods Rep 4-F3

Katz BG, Böhlke JK, Hornsby HD (2001) Timescales for nitrate contamination of spring waters, Northern Florida, USA. Chem Geol 179:167–186

Kaufmann G, Braun J (2000) Karst aquifer evolution in fractured, porous rocks. Water Resour Res 36:1381–1391

Land L, Huff GF (2010) Multi-tracer investigation of groundwater residence time in a karstic aquifer: bitter Lake national Wildlife Refuge, New Mexico, USA. Hydrogeol J 18:455–472

Land L, Timmons S (2016) Evaluation of groundwater residence time in a high mountain aquifer system (Sacramento Mountains, USA): insights gained from use of multiple environmental tracers. Hydrogeol J 24:787–804

Li XQ, Zhou AG, Liu CF, Cai HS (2007) SF6 age of karst water in Guilin. Carsologica Sin 26(3):207–211

Long AJ, Putnam LD (2006) Translating CFC-based piston ages into probability density functions of ground-water age in karst. J Hydrol 330(3–4):735–747

Long A, Sawyer J, Putnam L (2008) Environmental tracers as indicators of karst conduits in groundwater in South Dakota, USA. Hydrogeol J 16:263–280

Millero FJ (1986) The thermodynamics and kinetics of the hydrogen sulfide system in natural waters. Mar Chem 18(2–4):121–147

Morales T, Angulo B, Uriarte JA, Olazar M, Arandes JM, Antiguedad I (2017) Solute transport characterization in karst aquifers by tracer injection tests for a sustainable water resource management. J Hydrol 547:269–279

Plummer LN, Busenberg E, Böhlke JK, Nelms DL, Michel RL, Schlosser P (2001) Groundwater residence times in Shenandoah National Park, Blue Ridge Mountains, Virginia, USA: a multitracer approach. Chem Geol 179(1–4):93–111

Rose S, Long A (1988a) Monitoring dissolved oxygen in ground water: some basic considerations. Ground Water Monit Rev 8:93–97

Rose S, Long A (1988b) Monitoring dissolved oxygen in ground water: some basic considerations. Ground Water Monit Rem 8(1):93–97

Thayalakumaran T, Bristow KL, Charlesworth PB, Fass T (2008) Geochemical conditions in groundwater systems: implications for the attenuation of agricultural nitrate. Agric Water Manag 95(2):103–115

Yuan DX, Drogue C, Dai AD, Lao WK, Cai WT, Bidaux P, Razack M (1990) Hydrology of the karst aquifer at the experimental site of Guilin in southern China. J Hydrol 115(1–4):285–296

Yuan DX, Zhu DH, Weng JT et al (1991) Karst of China. Geologic Publishing House, Beijing

Yuan DX, Dai AD, Cai WT et al (1996) Karst water system of a peak cluster catchment in South China's bare karst region and its mathematic model. Guangxi Normal University Publishing House, Guilin

Zhu DH (1982) Evolution of peak cluster-depression in Guilin area and morphometric measurement. Carsologica Sin 2:127

Zoellmann K, Kinzelbach W, Fulda C (2001) Environmental tracer transport (H^3 and SF6) in the saturated and unsaturated zones and its use in nitrate pollution management. J Hydrol 240(3–4):187–205